Progress in simulating SOL plasma turbulence with the GBS code

P. Ricci[1], J. Morales[1], F. Nespoli[1], P. Paruta[1], F. Riva[1] , C. Wersal[1],
J.A. Boedo[2], I. Furno[1], F.D. Halpern[1], B. Labit[1], J. Loizu[3] , S. Jolliet[1],
R. Jorge[1], A. Mosetto[1], C. Tsui[2,1], the TCV Team, and the EUROfusion MST1 Team
[1] *EPFL, Swiss Plasma Center, CH-1015 Lausanne, Switzerland*
[2] *University of California - San Diego, La Jolla, California 92093, USA*
[3] *Max-Planck Institute for Plasma Physics, Wendelsteinstraβe 1, D-17491 Greifswald, Germany*

Introduction

Understanding the turbulent dynamics of the tokamak scrape-off layer (SOL) is one of the important scientific challenges to address as we approach the era of burning plasma experiments in magnetic fusion energy devices. The SOL plays a crucial role in determining the performance of tokamak devices, for instance, by controlling the impurity influx into the core plasma, the recycling level, and the heat exhaust.

The GBS code [1] was developed in the last few years to simulate plasma turbulence in SOL conditions. GBS advances the drift-reduced Braginskii equations for low-frequency plasma turbulence, solving at the same time a kinetic equation of neutral atoms by the method of characteristics. In the past, thanks to GBS simulations, we have significantly advanced our understanding of the mechanisms that regulate the SOL width, toroidal velocity, fluctuation amplitude, and electrostatic potential.

Recently, GBS simulations have allowed us to progress in the understanding of the role of shaping (e.g., elongation and triangularity) in setting the SOL width and of the physics mechanisms at play at the interface with the closed flux surface region. The simulation of the neutral atom dynamics has allowed us to shed light on the transition from the sheath to the conduction limited regime. We have carried out comparisons against TCV measurements, and we are also working on the development of a flexible numerical algorithm that will allow us to simulate SOL turbulence in diverted geometries. In the present abstract, we introduce the model equations to study the SOL plasma dynamics, the GBS numerical algorithm and, among the recent progress, we discuss the comparison with experiments carried out in the TCV tokamak [2].

Model equations

In the SOL the plasma dynamics results from the interplay of the plasma sources (due to the neutral ionization and the plasma outflow from the tokamak core), turbulent transport, and

plasma losses (at the limiter or divertor plates or through recombination processes). Therefore, a model has to evolve self-consistently both the plasma profile and its fluctuations, with no separation between the equilibrium and fluctuation scale lengths.

The perpendicular (turbulent) dynamics occurs on time scales longer than the ion cyclotron period, and it has length scales of the order of ρ_s, while the relevant length scale for the parallel dynamics is the magnetic field line length $\sim R$. Hence, it is advantageous to eliminate the undesired (fast) temporal scales, and to separate the parallel and the perpendicular dynamics. The required separation of temporal and spatial scales is achieved through the use of the following velocity representation:

$$\mathbf{v}_e = v_{\|e}\hat{\mathbf{b}} + \mathbf{v}_{\mathbf{E}\times\mathbf{B}} + \mathbf{v}_{\star,e} \tag{1}$$

$$\mathbf{v}_i = v_{\|i}\hat{\mathbf{b}} + \mathbf{v}_{\mathbf{E}\times\mathbf{B}} + \mathbf{v}_{\star,i} + \mathbf{v}_{\mathrm{pol},i} \tag{2}$$

together with the approximation $\mathbf{E} = -\nabla\phi - \hat{\mathbf{b}}_0\partial_t\psi$, where ψ represents the perturbed poloidal magnetic flux. The drift velocities $\mathbf{v}_{\mathbf{E}\times\mathbf{B}} = -\nabla\phi\times\hat{\mathbf{b}}_0/B$ and $\mathbf{v}_{\star,e,i} = -\nabla p_{e,i}\times\hat{\mathbf{b}}_0/(Z_{e,i}en_{e,i}B)$ are the zeroth order solution to the perpendicular component of the moment equations, $\hat{\mathbf{b}}$ is a unit vector in the direction of the magnetic field and $\hat{\mathbf{b}}_0$ its equilibrium direction. The ion polarization drift $\mathbf{v}_{\mathrm{pol},i}$ is obtained as a first order correction to $\mathbf{v}_i$.

We retain an equation for the electron density, a vorticity equation that enforces charge conservation, and equations for the ion and electron temperatures and parallel velocities:

$$\frac{\partial n}{\partial t} = -\frac{1}{B}[\phi,n] - \nabla(nv_{\|\mathrm{e}}\hat{\mathbf{b}}) + \frac{2}{eB}\left[C(p_\mathrm{e}) - enC(\phi)\right] + \mathscr{D}_\mathrm{n}(n) + S_\mathrm{n} + n_\mathrm{n}\nu_\mathrm{iz} - n\nu_\mathrm{rec} \tag{3}$$

$$\frac{\partial\tilde{\omega}}{\partial t} = -\frac{1}{B}[\phi,\tilde{\omega}] - v_{\|\mathrm{i}}\nabla_\|\tilde{\omega} + \frac{B^2}{m_\mathrm{i}n}\nabla(j_\|\hat{\mathbf{b}}) + \frac{2B}{m_\mathrm{i}n}C(p) + \mathscr{D}_{\tilde{\omega}}(\tilde{\omega}) - \frac{n_\mathrm{n}}{n}\nu_\mathrm{cx}\tilde{\omega} \tag{4}$$

$$\begin{aligned}\frac{\partial v_{\|\mathrm{e}}}{\partial t} + \frac{e}{m_\mathrm{e}}\frac{\partial\Psi}{\partial t} = &-\frac{1}{B}[\phi,v_{\|\mathrm{e}}] - v_{\|\mathrm{e}}\nabla_\|v_{\|\mathrm{e}} + \frac{e}{\sigma_\|m_\mathrm{e}}j_\| + \frac{e}{m_\mathrm{e}}\nabla_\|\phi - \frac{T_\mathrm{e}}{m_\mathrm{e}n}\nabla_\|n - \frac{1.71}{m_\mathrm{e}}\nabla_\|T_\mathrm{e} + \mathscr{D}_{v_{\|\mathrm{e}}}(v_{\|\mathrm{e}}) \\ &+ \frac{n_\mathrm{n}}{n}(\nu_\mathrm{en} + 2\nu_\mathrm{iz})(v_{\|\mathrm{n}} - v_{\|\mathrm{e}})\end{aligned} \tag{5}$$

$$\begin{aligned}\frac{\partial v_{\|\mathrm{i}}}{\partial t} = &-\frac{1}{B}[\phi,v_{\|\mathrm{i}}] - v_{\|\mathrm{i}}\nabla_\|v_{\|\mathrm{i}} - \frac{1}{m_\mathrm{i}n}\nabla_\|p + \mathscr{D}_{v_{\|\mathrm{i}}}(v_{\|\mathrm{i}}) \\ &+ \frac{n_\mathrm{n}}{n}(\nu_\mathrm{iz} + \nu_\mathrm{cx})(v_{\|\mathrm{n}} - v_{\|\mathrm{i}})\end{aligned} \tag{6}$$

$$\frac{\partial T_\mathrm{e}}{\partial t} = -\frac{1}{B}[\phi, T_\mathrm{e}] - v_{\parallel \mathrm{e}}\nabla_\parallel T_\mathrm{e} + \frac{4T_\mathrm{e}}{3eB}\left[\frac{T_\mathrm{e}}{n}C(n) + \frac{7}{2}C(T_\mathrm{e}) - eC(\phi)\right] \tag{7}$$
$$+ \frac{2T_\mathrm{e}}{3n}\left[\frac{0.71}{e}\nabla(j_\parallel \hat{\mathbf{b}}) - n\nabla(v_{\parallel \mathrm{e}}\hat{\mathbf{b}})\right] + \mathscr{D}_{T_\mathrm{e}}(T_\mathrm{e}) + \mathscr{D}^{\parallel}_{T_\mathrm{e}}(T_\mathrm{e}) + S_{T_\mathrm{e}}$$
$$+ \frac{n_\mathrm{n}}{n}\nu_\mathrm{iz}\left[-\frac{2}{3}E_\mathrm{iz} - T_\mathrm{e} + m_\mathrm{e}v_{\parallel \mathrm{e}}\left(v_{\parallel \mathrm{e}} - \frac{4}{3}v_{\parallel \mathrm{n}}\right)\right] - \frac{n_\mathrm{n}}{n}\nu_\mathrm{en}m_\mathrm{e}\frac{2}{3}v_{\parallel \mathrm{e}}(v_{\parallel \mathrm{n}} - v_{\parallel \mathrm{e}})$$
$$\frac{\partial T_\mathrm{i}}{\partial t} = -\frac{1}{B}[\phi, T_\mathrm{i}] - v_{\parallel \mathrm{i}}\nabla_\parallel T_\mathrm{i} + \frac{4T_\mathrm{i}}{3eB}\left[C(T_\mathrm{e}) + \frac{T_\mathrm{e}}{n}C(n) - \frac{5}{2}C(T_\mathrm{i}) - eC(\phi)\right] \tag{8}$$
$$+ \frac{2T_\mathrm{i}}{3n}\left[\frac{1}{e}\nabla(j_\parallel \hat{\mathbf{b}}) - n\nabla(v_{\parallel \mathrm{i}}\hat{\mathbf{b}})\right] + \mathscr{D}_{T_\mathrm{i}}(T_\mathrm{i}) + \mathscr{D}^{\parallel}_{T_\mathrm{i}}(T_\mathrm{i}) + S_{T_\mathrm{i}}$$
$$+ \frac{n_\mathrm{n}}{n}(\nu_\mathrm{iz} + \nu_\mathrm{cx})\left[T_\mathrm{n} - T_\mathrm{i} + \frac{1}{3}(v_{\parallel \mathrm{n}} - v_{\parallel \mathrm{i}})^2\right]$$

with $p = n(T_\mathrm{e} + T_\mathrm{i})$, the total pressure, and $\sigma_\parallel = 1.96e^2 n\tau_\mathrm{e}/m_\mathrm{e}$, the parallel conductivity, where τ_e is the electron collision time. The generalized vorticity, $\tilde{\omega} = \omega + 1/e\nabla^2_\perp T_\mathrm{i}$, is related to the electrostatic potential by $\nabla^2_\perp \phi = \omega$, while $(\beta_{\mathrm{e}0}/2)\nabla^2_\perp \Psi = j_\parallel$, with $\beta_{\mathrm{e}0} = 2\mu_0 p_\mathrm{e}/B^2$ and $j_\parallel = n\left(v_{\parallel i} - v_{\parallel e}\right)$. The following operators have been introduced $\nabla_\parallel A = \hat{\mathbf{b}}\cdot\nabla A$, $[A,B] = \hat{\mathbf{b}}_0 \cdot (\nabla A \times \nabla B)$, and $C(A) = B/2[\nabla \times (\hat{\mathbf{b}}_0/B)]\cdot\nabla A$. The ionization, recombination, elastic electron-neutral, and charge-exchange processes are described, respectively, through the use of Krook operators with collision frequencies defined as $\nu_\mathrm{iz} = n_e\langle v_e\sigma_\mathrm{iz}(v_e)\rangle$, $\nu_\mathrm{rec} = n_e\langle v_e\sigma_\mathrm{rec}(v_e)\rangle$, $\nu_\mathrm{en} = n_e\langle v_e\sigma_\mathrm{en}(v_e)\rangle$, $\nu_\mathrm{cx} = n_i\langle v_i\sigma_\mathrm{cx}(v_i)\rangle$ where σ_iz, σ_rec, σ_en and σ_cx, are the ionization, recombination, elastic electron-neutral, and charge-exchange cross sections. The neutral atoms dynamics is obtained by solving the kinetic equation

$$\frac{\partial f_\mathrm{n}}{\partial t} + \mathbf{v}\cdot\frac{\partial f_\mathrm{n}}{\partial \mathbf{x}} = -\nu_\mathrm{iz}f_\mathrm{n} - \nu_\mathrm{cx}\left(f_\mathrm{n} - \frac{n_\mathrm{n}}{n_i}f_i\right) + \nu_\mathrm{rec}f_i. \tag{9}$$

In Eq. (4), the polarization velocity and its divergence retain corrections due to density gradients, *i.e.* the commonly used Boussinesq approximation is avoided. The source terms S_n, S_{T_e}, and S_{T_i} have been added to the density and temperature equations to model the outflow of hot plasma from the core to the SOL. A detailed study of the interaction of the plasma with the solid wall was carried out and, based on the kinetic results, a set of boundary conditions was found, implemented in GBS at the sheath edge.

Numerical implementation

A radial section of a torus, with coordinate system $(y = a\theta, x, \varphi)$ is mapped to a discrete Cartesian grid. The φ coordinate is periodic, while periodicity in y can be selected for a chosen range of x – thus, we can vary between a poloidally periodic plasma, a limited plasma, or we can mix open and closed field lines. Time integration is carried out with the Runge-Kutta order 4 algorithm.

Spatial gradients are computed using standard second order centered finite difference formulas, while the $\mathbf{E} \times \mathbf{B}$ non-linear advection terms are discretized using the Arakawa scheme. The Poisson and Ampère equations can be solved using sparse matrix methods, or using a stencil-based multigrid solver. The kinetic equation for the neutral atoms is solved by using the method of the characteristics.

Comparison with TCV experiments

GBS simulation have been carried out in a circular inboard-limited ohmic L-mode discharge, the plasma current and the toroidal magnetic field on axis being respectively $I_p = 145$ kA and $B_\phi = 1.45$ T. The values of the plasma density and temperature at the LCFS, $n_{e,0} = 5 \times 10^{18}$ m^{-3} and $T_{e,0} = 25$ eV, are deduced from Langmuir probes embedded in the limiter.

Figure 1 shows the resulting heat flux profile for one of the two limiters and the comparison with the experimental profile. Both the experimental and the simulated parallel heat flux radial profiles on the limiter are well described by a sum of two exponentials $q_{||} = q_s \exp(-r_u/\lambda_s) + q_l \exp(-r_u/\lambda_l)$ where r_u is the upstream coordinate (with $r_u = 0$ at the LCFS).

The fitted values for the simulation, $\lambda_s = 2.9$ mm (2.8 mm) and $\lambda_l = 37$ mm (39 mm) for the upper (lower) limiter respectively, are in quantitative agreement with the experimental ones obtained by means of infrared thermography $\lambda_{s,IR} = 3.2$ mm, $\lambda_{l,IR} = 37$ mm (the infrared analysis was possible only for the upper part of the limiter). Nevertheless, the relative importance of the near SOL q_s/q_l is much smaller in the simulation than in the experiment.

This research was supported in part by the Swiss National Science Foundation and was carried out within the framework of the EUROfusion Consortium. It received funding from the Euratom research and training programme 2014-2018 under grant agreement No 633053. The views and opinions expressed herein do not necessarily reflect those of the European Commission.

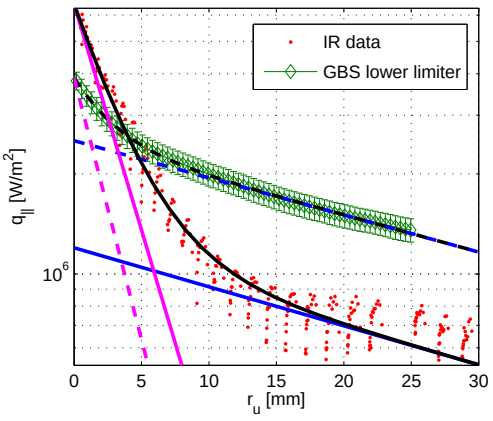

Figure 1: *Comparison of GBS results with TCV infra-red measurements of the heat flux at the vessel wall in a limited discharge.*

References

[1] P. Ricci, et al., Plasma Phys. Contr. Fusion **54**, 124047 (2012); F. Halpern et al., J. Comp. Phys. **315**, 388 (2016).

[2] F. Nespoli et al., J. Nucl. Mat. & En., submitted (2016).